Insights into the Mechanism of O−2 Formation and Release from the Mn4O4L6 "Cubane" Cluster

ARTICLE *in* THE JOURNAL OF PHYSICAL CHEMISTRY A · OCTOBER 2010

Impact Factor: 2.69 · DOI: 10.1021/jp105422a · Source: PubMed

Insights into the Mechanism of O_2 Formation and Release from the $Mn_4O_4L_6$ "Cubane" Cluster

Aleksey E. Kuznetsov, Yurii V. Geletii, Craig L. Hill, and Djamaladdin G. Musaev*

Cherry L. Emerson Center for Scientific Computation and Department of Chemistry, Emory University, 1515 Dickey Drive, Atlanta, Georgia 30322, United States

Received: June 13, 2010; Revised Manuscript Received: August 5, 2010

To probe photoinduced water oxidation catalyzed by the $Mn_4O_4L_6$ cubane clusters, we have computationally studied the mechanism and controlling factors of the O_2 formation from the $[Mn_4O_4L_6]$ catalyst, **6**. It was demonstrated that dissociation of an $L = H_2PO_2^-$ ligand from **6** facilitates the direct O−O bond formation that proceeds with a 28.3 (33.4) kcal/mol rate-determining energy barrier at the transition state **TS1**. This step (the O−O single bond formation) of the reaction is a two-electron oxidation/reduction process, during which two oxo ligands are transformed into to μ^2:η^2−O_2^{2-} unit, and two ("distal") Mn centers are reduced from the 4+ to the 3+ oxidation state. Next two-electron oxidation/reduction occurs by "dancing" of the resulted O_2^{2-} fragment between the Mn^1 and Mn^2/$Mn^{2'}$-centers, keeping its strong coordination to the $Mn^{1'}$-center. As a result of this four-electron oxidation/reduction process Mn centers of the Mn_4-core of **I** transform from $\{Mn^1(III)\text{-}Mn^{1'}(III)\text{-}Mn^2(IV)\text{-}Mn^{2'}(IV)\}$ to $\{Mn^1(II)\text{-}Mn^{1'}(II)\text{-}Mn^2(III)\text{-}Mn^{2'}(III)\}$ in **IV**. In other words, upon O_2 formation in cationic complex $[Mn_4O_4L_5]^+$, **I**, all four Mn-centers are reduced by one electron each. The overall reaction **I** → **TS1** → **II** → **III** → **TS2** → **IV** → **TS3** → **V** → **VI** + $\mathbf{O_2}$ is found to be exothermic by 15.4 (10.5) kcal/mol. We analyze the lowest spin states and geometries of all reactants, intermediates, transition states, and products of the targeted reaction.

I. Introduction

The development of efficient photodriven systems that convert solar energy to chemical energy by splitting water into O_2 and H_2 is a core and monumental challenge in renewable energy research.[1,2] In general, photodriven systems contain three major components: photosensitizer, water oxidation catalyst (WOC), and hydrogen evolving/formation catalyst (HEC),[2] and no component aspect in designing these radiant energy conversion systems is more challenging than development of a viable WOC. The ideal WOC must be fast, amenable to interfacing with sensitizer materials of various kinds, and stable to oxidative, hydrolytic, and thermal degradation during catalytic turnover. Furthermore, it should exhibit several electron transfer (ET) or proton-coupled electron transfer (PCET) events over a narrow potential range (redox leveling), facilitating water oxidation/oxygen evolution near the thermodynamic potential.

Currently, research activity on water oxidation catalysts is at a record level of activity. To date, several Ru-based complexes,[3−20] starting with the famous "blue dimer" of Meyer,[3,15] several Mn-based,[21−36] and three organometallic[37−39] homogeneous WOCs have been reported. In addition, numerous heterogeneous[40−48] WOCs are known. To this end, we recently reported three catalysts $[\{Ru_4O_4(OH)_2(H_2O)_4\}(\gamma\text{-}SiW_{10}O_{36})_2]^{10-}$, **1**;[49−51] (simultaneously and independently, Bonchio and co-workers[52,53] prepared a different salt of this polyanion via another synthetic route), $[\{Ru_4O_5(OH)(H_2O)_4\}(\gamma\text{-}PW_{10}O_{36})_2]^{9-}$, **2**;[54] and $[Co_4(H_2O)_2(\alpha\text{-}PW_9O_{34})_2]^{10-}$, **3**;[55] free of organic moieties, that exhibit several reversible one-electron redox couples by cyclic voltammetry and catalyze both the electrooxidation and chemical oxidation of water in aqueous solution at low overpotentials. Two other related complexes have also been reported: $K_{14}[(IrCl_4)KP_2W_{20}O_{72}]$, **4**,[56] a fast oxidatively resistant WOC that, unlike **1**−**3**, is not hydrolytically stable; and (b) $[(CH_3)_2NH_2]_{5.33}H_2[(\alpha\text{-}P_2W_{15}O_{56})Mn^{III}_3Mn^{IV}O_3(CH_3COO)_3]^{8-}$, **5**,[57] a POM complex with a Mn_4-core that shows limited water oxidation activity. Recent mechanistic studies[58−85] of the WOCs have clarified several issues important for WOC optimization. However, for improvement of the efficiency of the existing WOCs, as well as discovery of more efficient and stable WOCs, it is vital to elucidate the fundamental elementary processes taking place during water oxidation catalyzed by various WOCs and to clarify the factors affecting the efficiency of these steps. One such process is O−O bond formation in these systems, which could well proceed via different mechanisms with different WOCs. Indeed, as shown in the literature,[58−85] O_2 formation during the water oxidation by WOCs could occur via either a direct O−O coupling mechanism or an external water assisted pathway that includes (a) HO−H bond activation by two O-centers (those that are ligated to transition metal center(s) and oxidized with likely associated deprotonation of the coordinated water molecules) and formation of a complex with HOO^- and HO^- ligands, (b) H-atom transfer from the HOO^- ligand to the OH^- ligand to form an aqua-peroxo complex with O_2 and H_2O ligands, and (c) dissociation of the resulting O_2 molecule. However, factors controlling the mechanism of these important elementary reactions still remain unclear. Joint experimental and computational efforts to establish the mechanisms of the water oxidation to O_2 catalyzed by **1** and **2** have been published,[49−51] and others are in progress. Here, we report computational studies on the formation and release of O_2 from the $[Mn_4O_4L_6]$-catalyst (where $L = \{p\text{-}MeOPh)_2PO_2\}_6$), **6**, reported by Dismukes and co-workers.[30−33] We hope that understanding of O_2 formation in this Mn_4O_4-core will help to improve the efficiency of our

* To whom correspondence should be addressed. E-mail: dmusaev@emory.edu.

10.1021/jp105422a
Published on Web 10/06/2010

SCHEME 1

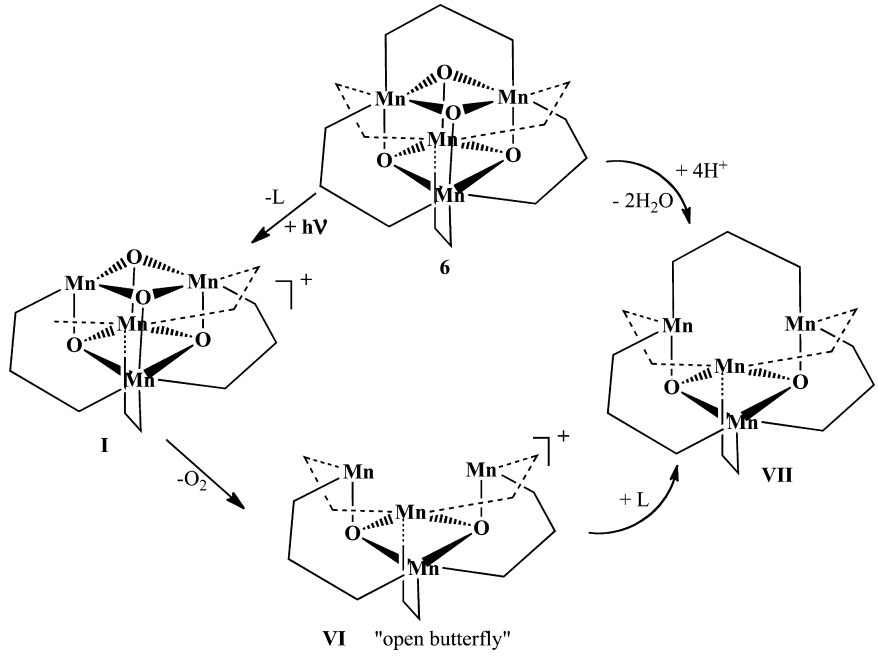

oxidatively and hydrolytically stable POM WOC, **5**, that also contains the Mn_4-cluster.[57]

Briefly, extensive studies of Dismukes and co-workers[30−36] have demonstrated that two of the four equivalent oxygen atoms in the Mn_4O_4 core of the cube-like complex $[Mn_4O_4L_6]$, **6**, where L = diarylphosphinates $R_2PO_2^-$, undergo reduction by a proton-coupled electron-transfer (PCET) reaction to yield two water molecules *in solution*. This process is reported to be readily reversible. On the basis of these studies, the authors concluded that the oxygen bridges in the **6** form from water. Furthermore, it was shown that **6** releases molecular O_2 when triggered by the photodissociation of one phosphinate ligand upon illumination *in the gas phase*. Photodissociation is quenched in condensed phases, resulting in minimal O_2 release. Photodissociation of one phosphinate ligand generates the $[Mn_4O_4L_5]^+$ complex, **I**, which transforms to the $[Mn_4O_2L_5]^+$ "butterfly" complex after the formation and release of O_2 (see Scheme 1). Recoordination of the ligand L, at the following stage, leads to the formation of a $[Mn_4O_2L_6]$ complex that can also be generated in solution from **6** via reduction of two O-centers by a proton-coupled electron-transfer (PCET) reaction to yield two water molecules. However, elucidation of the mechanism and controlling factors of the reaction given in Scheme 1 requires a comprehensive experimental and computational study. Here, we report our computational findings on the mechanism of this reaction.

It is noteworthy that electronic structure of the complexes $[Mn_4O_4L_6]$ with L = diphenylphosphinate (**6a**) and bis(4-methoxyphenyl)phosphinate (**6b**) were the subject of previous DFT studies.[32a] In these calculations, relatively small (3-21G* for Mn, O, and P atoms, and 3-21G for C and H atoms) basis sets were used. The geometry of **6a** was optimized at the fixed T_d symmetry of the molecule, whereas the electronic structure of **6b** was calculated at the geometry fixed to that for optimized **6a** (by replacing the para H atoms in the phenyl rings of $Ph_2PO_2^-$ ligands by MeO groups). It was shown that the ligand dissociation from **6b** is much easier (by 14.7 kcal/mol) than from **6a**.

Dismukes and co-workers[36b] also proposed a mechanism similar to that presented in Scheme 1 without reporting any geometry features and relative energies of the assumed intermediates.

II. Computational Details

All calculations were performed using the Gaussian_03 program.[86] The geometries of all species under investigation were optimized without any symmetry constraint at the B3LYP/Lanl2dz level of theory with additional d polarization functions for the P atom ($\alpha = 0.55$) and the corresponding Hay-Wadt effective core potentials (ECPs) for Mn.[87,88] This method is subsequently referred to as the "B3LYP/[Lanl2dz + d(P)]" approach. For all species under investigation, Hessians were calculated, and all transition states were confirmed to have one imaginary frequency corresponding to the reaction coordinates. The solvent effects were estimated at the B3LYP/[Lanl2dz + d(P)] level of theory using the self-consistent reaction field IEF-PCM method[89] (UA0 model) with water as a solvent (dielectric constant $\epsilon = 78.39$). We used the $H_2PO_2^-$ ion as a model for a ligand L^-.

Below, we discuss gas-phase Gibbs free energetics (ΔG) calculated at the B3LYP//[Lanl2dz+d(P)] level of theory. The energies including solvent effects ($\Delta G + \Delta G_{solv}$) are provided in parentheses. The Cartesian coordinates of all optimized structures at the B3LYP/[Lanl2dz+d(P)] level are presented in the Supporting Information.

III. Results and Discussion

A. Reactants. Dismukes and co-workers[31,32,36b] proposed the positively charged cluster $Mn_4O_4L_5^+$, **I**, to be a reactant species for O_2 formation. This complex can be generated from the neutral compound $Mn_4O_4L_6$, **6**, by photodissociation of one of the L ligands:

$$Mn_4O_4L_6,\mathbf{6} + h\nu \rightarrow Mn_4O_4L_{5+},\mathbf{I} + L^- \qquad (1)$$

Since both the neutral **6** and cationic **I** complexes are expected to have two Mn(III) and two Mn(IV) centers, they may have several lower-lying spin states. Careful evaluation of all possible spin states (see Supporting Information for more details) showed that both species possess high-spin ^{15}A ground electronic states (in C_1 symmetry) with 14 unpaired spins. As seen in Table 1,

TABLE 1: Calculated Mulliken Spin Densities (In e) and $\langle S^2 \rangle$ Values of the Studied Derivatives of the $Mn_4O_4L_6$ (L = H_2PO_2) Complex

atoms	**6** $^{15}A(^7A)$	**I** $^{15}A(^7A)$	**TS1** ^{17}A	**II** $^{17}A(^9A)$	**III** ^{19}A	**TS2** ^{19}A	**IV** ^{19}A	**TS3** ^{19}A	**V** ^{17}A	**VI** ^{19}A	**VII** ^{19}A
Mn^1	3.91 (2.89)	3.85 (3.85)	3.94	3.96 (3.84)	4.77	4.70	4.77	4.78	4.78	4.82	4.77
$Mn^{1'}$	3.91 (−3.90)	3.85 (−3.82)	3.84	4.02 (4.05)	3.92	4.39	4.73	4.71	4.69	4.84	4.77
Mn^2	3.10 (3.10)	3.01 (3.01)	3.59	3.89 (−3.82)	3.87	3.83	3.88	3.88	3.89	3.94	3.94
$Mn^{2'}$	3.10 (3.10)	3.01 (3.01)	3.86	3.88 (3.84)	3.87	3.90	3.51	3.83	3.88	3.94	3.94
O^1	−0.13 (−0.07)	−0.13 (−0.06)	−0.07	−0.11 (−0.16)	0.61	0.42	0.34	0.08	−1.07		
$O^{1'}$	−0.13 (−0.07)	−0.13 (−0.06)	0.51	−0.04 (−0.03)	0.52	0.50	0.22	0.10	−0.84		
O^2	−0.17 (−0.14)	−0.02 (−0.04)	−0.14	−0.09 (0.03)	−0.04	−0.15	0.00	0.01	0.03	0.02	−0.02
$O^{2'}$	−0.17 (−0.17)	−0.02 (−0.04)	−0.06	−0.06 (0.07)	−0.05	−0.20	−0.06	−0.01	0.03	0.01	−0.02
$\langle S^2 \rangle$	56.4 (15.9)	56.3 (15.9)	72.2	72.4	90.2	90.4	90.5	90.9	72.4	90.1	90.1

in the ^{15}A ground states of these complexes, two Mn centers, Mn^1 and $Mn^{1'}$, bear approximately four unpaired electrons each (α-spin), whereas Mn^2 and $Mn^{2'}$ centers have approximately three unpaired electrons each (α-spin). All Mn centers are ferromagnetically coupled. Thus, Mn^1 and $Mn^{1'}$ centers should be considered as having oxidation state 3+, and Mn^2 and $Mn^{2'}$ centers as having oxidation state 4+. It is worthwhile to remark that the O centers of the Mn_4O_4 core bear small amounts of unpaired spin densities, 0.13e (β-spin) on $O^1/O^{1'}$ and 0.17e (β-spin) on $O^2/O^{2'}$ (see Table 1).

Intermediate-spin states of these complexes with eight unpaired spins, that is, ^9A states, lie only 2.6 (−0.1) kcal/mol higher (lower) for $Mn_4O_4L_6$ and 2.5 (10.6) kcal/mol higher for $Mn_4O_4L_5^+$. It is interesting to note that septet ^7A states of both compounds with antiferromagnetically coupled Mn^1 and $Mn^{1'}$ centers lie energetically very close to their ^{15}A ground electronic states. For **6**, the ^7A state was calculated to be 2.1 kcal/mol higher in the gas-phase and 0.7 kcal/mol lower in the aqueous solution than the ^{15}A state, whereas for **I** the ^7A state was calculated to be only 0.3 kcal/mol lower in the gas-phase and 0.3 kcal/mol higher in the aqueous solution than the ^{15}A state. Interestingly, the antiferromagnetic coupling of spins of Mn^1 and $Mn^{1'}$ centers does not effect the geometries of both compounds calculated for their ^{15}A states. The located structures of **6** and **I** are given in Figure 1, and their important geometric parameters in their ^{15}A ground electronic states are given in Table 2. The full geometries of these species (in their several lower-lying electronic states) are provided in Supporting Information. It is worthwhile to note that the antiferromagnetic coupling of spins of Mn^1 and $Mn^{1'}$ centers only slightly changes spin densities on the O centers of the Mn_4O_4 core (see Table 1). Furthermore, due to geometry similarities and nonsignificant energy differences between the ^{15}A, ^9A, and ^7A electronic states (see Supporting Information) of complexes **6** and **I**, we will discuss below, in sake of simplicity, only the high-spin states of the these systems.

On the basis of the ground state-to-ground state principle, reaction 1 is found to be endothermic by 147.4 and (41.7) kcal/mol in the gas-phase and water solution, respectively.

Analysis of the geometry parameters (see Figure 1 and Table 2) of the neutral species **6** shows that its ^{15}A state possesses symmetry quite close to C_{2v}. The calculated Mn^2-O^1 ($Mn^{2'}-O^{1'}$), Mn^1-O^2 ($Mn^{1'}-O^{2'}$), Mn^1-O^1 ($Mn^{1'}-O^{1'}$), $Mn^1-O^{1'}$ ($Mn^{1'}-O^1$), and $Mn^2-O^{2/2'}$ ($Mn^{2'}-O^{2/2'}$) bond distances are 1.87 (1.87), 2.04 (2.05), 1.89 (1.88), 2.36 (2.35), and 1.91(1.93) Å, respectively. As seen from the table, the calculated geometry parameters are in reasonable agreement with their experimental values reported for the neutral $[Mn_4O_4\{p\text{-}MeOPh)_2PO_2\}_6]$ species.[32b] The computed $O^1-O^{1'}$ and $O^2-O^{2'}$ distances, 2.74 and 2.47 Å, and their measured[32b] values of 2.727(2) and 2.484(2), are significantly longer than the experimental value for the free O_2 molecule (1.21 Å),[90] for O_2^- (1.35 Å)[91] and the calculated values of 1.64 Å (with the SD-CI approach) and 1.67 Å (with the SAC−CI approach)[92] for O_2^{2-}. Thus, effectively no O−O bond exists in **6**. This conclusion is also in good agreement with the experiments of Dismukes and co-workers.[32b]

As seen in Figure 1 and Table 2, the ^{15}A ground state of **I** possesses C_s or very close to C_s symmetry. Comparison of the geometries of **6** and **I** shows the following changes upon dissociation of the $L^- = H_2PO_2^-$ ligand from the precursor species **6:** (a)

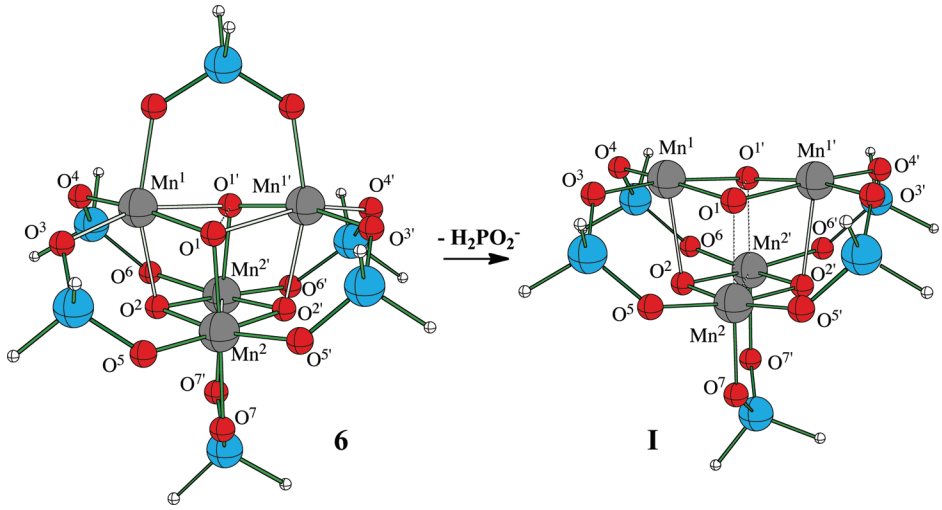

Figure 1. The optimized structures of the neutral $Mn_4O_4L_6$ species, **6**, and the cationic $Mn_4O_4L_5^+$ species, **I**. Table 2 includes the calculated important geometry parameters for these species.

TABLE 2: Calculated Important Geometry Parameters (In Å) of the: (a) Neutral $Mn_4O_4L_6$ Species, 6; (b) Cationic $Mn_4O_4L_5^+$ Species, I; and (c) Intermediates, Transition States and Products of the O_2 Formation and Release from the Cationic $Mn_4O_4L_5^+$ Species, I[a]

structures	Mn^1-O^1	$Mn^1-O^{1'}$	$Mn^{1'}-O^1$	$Mn^{1'}-O^{1'}$	Mn^1-O^2	$Mn^{1'}-O^{2'}$	Mn^2-O^1	$Mn^{2'}-O^{1'}$	Mn^2-O^2	$Mn^2-O^{2'}$	$Mn^{2'}-O^2$	$Mn^{2'}-O^{2'}$	$O^1-O^{1'}$
6	1.89	2.36	2.35	1.88	2.04	2.05	1.87	1.87	1.91	1.91	1.93	1.93	2.74
exp[b]	1.8747	2.2269	2.2269	1.8747	1.9358	1.9358	1.8282	1.8282	1.8918	1.8918	19029	1.9029	2.747
I	1.94	1.94	1.94	1.94	2.15	2.16	2.00	2.00	1.89	1.89	1.89	1.89	2.45
TS1	2.67	2.12	1.88	1.90	1.80	2.25	2.08	3.48	1.98	1.92	2.23	1.86	1.85
II	2.86	2.17	1.89	2.01	1.79	2.20	2.55	3.55	2.00	1.92	2.22	1.86	1.50
III		2.27	2.20		2.12	1.79	3.67	2.55	1.88	2.19	1.94	1.97	1.38
TS2		2.26	2.24		2.05	1.90	2.60	3.54	1.90	2.02	1.93	1.98	1.37
IV			2.31		2.00	2.03		2.17	1.95	1.93	1.90	1.90	1.32
TS3			2.39		2.00	1.99		2.70	1.94	1.91	1.91	1.93	1.28
V			2.24		2.00	2.00			1.92	1.92	1.92	1.93	1.27
VI					2.00	2.00			1.92	1.92	1.92	1.92	

[a] For notations of the presented geometrical parameters and structures, see Figure 2. [b] See ref 32b.

the $O^1-O^{1'}$ distance is shortened by 0.29 Å, which implies increasing feasibility of $O^1-O^{1'}$ bond formation in **I**; (b) Mn^1-O^2/$Mn^{1'}-O^{2'}$ bond distances are shortened by 0.11 Å; (c) Mn^2-O^2/$^{2'}$ and $Mn^{2'}-O^2$/$^{2'}$ bond distances are shortened by 0.04 and 0.02 Å, respectively; and (d) $Mn^1-Mn^{1'}$ and $Mn^2-Mn^{2'}$ distances are shortened by 0.26 and 0.03 Å, respectively. The $Mn^1-O^{1/1'}$ ($Mn^{1'}-O^{1/1'}$) bond distances are noticeably equalized, all being *ca.* 1.94 Å. Thus, the whole Mn_4O_4 core becomes more compact upon ligand dissociation from **6**, which is rationalized by increased positive charge on the resulting species, **I**. On the basis of these geometrical changes one may conclude that upon the ligand dissociation from **6** the interactions within two (top and bottom) Mn_2O_2 halves (including $Mn^{1/1'}-O^{1/1'}$ and $Mn^{2/2'}-O^{2/2'}$, respectively) of the Mn_4O_4-core are increased, whereas the interactions between these two Mn_2O_2-halves of the Mn_4O_4-core are decreased. The Mulliken spin analysis shows that the spin distribution does not change significantly upon the ligand dissociation from **6**.

In summary, dissociation of $L^- = H_2PO_2^-$ ligand from the species **6** (a) makes the Mn_4O_4-core more compact; (b) significantly shortens the $O^1-O^{1'}$ distance, which facilitates the $O^1-O^{1'}$ bond formation; and (c) does not change significantly the spin distribution in the Mn_4O_4-core.

The calculated intermediates and transition states involved in the formation and release of O_2 from **I** are presented in Figure 2. Their important geometry parameters are given in Table 2. For simplicity of our discussion, we divide this process into the following two subprocesses: (i) O−O ($O^1-O^{1'}$) bond formation, **I** → **TS1** → **II**; and (ii) O_2 ($O^1-O^{1'}$) release and formation of reduced $Mn_4O_2L_5^+$ species, **II** → **III** → **TS2** → **IV** → **TS3** → **V** → **VI** + O_2. Below, we discuss each of these steps in more detail.

B. O−O Bond Formation. This step of the targeted reaction starts from the reactant **I** and proceeds via the transition state **TS1**, which is confirmed to be a real transition state (with one imaginary frequency of 769 cm^{-1}) that connects reactant **I** and product **II**. As seen in Figure 2 and Table 2, the geometry of the Mn_4O_4 core is strongly distorted at **TS1** compared with that of the reactant **I**: (a) the Mn^1-O^1 and $Mn^{2'}-O^{1'}$ bond distances are significantly elongated, by 0.73 and 1.48 Å, respectively, and, thus these Mn−O bonds can be considered as broken in **TS1**, whereas the $Mn^{1'}-O^{1/1'}$ and Mn^2-O^1 bond distances are only slightly (within 0.06−0.08 Å range) changed; (b) the $Mn^{1'}-O^{2'}$ and Mn^1-O^2 bond distances are elongated by 0.09 and shortened by 0.25 Å, respectively; (c) $Mn^{2'/2}-O^2$ bond distances are elongated by 0.34 and 0.09 Å, respectively; and (d) the $O^1-O^{1'}$ bond distance is shortened by 0.6 Å, which indicates the beginning of the O−O ($O^1-O^{1'}$) bond formation. These geometry changes are clearly associated with the $O^1-O^{1'}$ single bond formation and transfer of the resulting O_2 unit to the $Mn^{1'}$ center.

The Mulliken spin analysis (see Table 1) shows that in **TS1** the Mn^1 and $Mn^{1'}$ centers still bear about four unpaired electrons each (α-spin), thus retaining the oxidation state 3+, as in the reactant species **I**. In contrast, the spin distribution change in the Mn^2 and $Mn^{2'}$ centers is remarkable: indeed, at **TS1**, (a) the Mn^2-center has about 3.60e of unpaired spin-density (α-spin), compared to 3.01e in **I**, and therefore could be considered as having an intermediate oxidation state 3+/4+; and (b) the $Mn^{2'}$ center bears about four (3.86) unpaired electrons (α-spin) compared to 3.01e in **I**, and therefore could be considered as having oxidation state 4+. The resulting $O^1-O^{1'}$ unit in **TS1** bears 0.44e of α-spin density. The total spin density on O^2 and $O^{2'}$ centers also increases up to 0.20e of β-spin density compared to 0.04e of β-spin density in **I**.

Thus, in **TS1,** the 1-electron reduction of the Mn^2 and $Mn^{2'}$ atoms has started and the required electrons for this process are provided by the O^1 and $O^{1'}$ atoms. The energy barrier, calculated as the energy difference between the reactant **I** and **TS1,** is found to be 28.3 (33.4) kcal/mol. Passing over **TS1** leads to the formation of intermediate **II** with the O_2^{2-} unit. The resulting structure **II** lies 9.7 (13.9) kcal/mol higher in energy than reactant **I**, in its ground ^{17}A electronic state.

Close inspection geometry of **II** shows further shortening of the $O^1-O^{1'}$ bond distance to 1.50 Å, which is close to the value of 1.475 Å found in the H_2O_2 molecule.[90] In **II**, (a) the $Mn^1-O^{1/1'}$ bond distances are longer by 0.92 and 0.23 Å, respectively; (b) the $Mn^{1'}-O^1$ and $Mn^{1'}-O^{1'}$ bond distances are shorter by 0.05 Å and elongated by 0.07 Å, respectively; (c) the Mn^2-O^1 and $Mn^2-O^{1'}$ distances are longer by 0.55 and 1.55 Å, respectively; (d) the Mn^1-O^2 and $Mn^{1'}-O^{2'}$ bond distances are shorter by 0.36 Å and longer by 0.04 Å, respectively; and (e) the $Mn^{2/2'}-O^2$ bond distances are longer by 0.11 and 0.33 Å, respectively, compared to **I**.

In general in **II**, the Mn_4O_4 core is strongly distorted relative to that in the reactant **I**. In **II**, the $O^1-O^{1'}$ unit is coordinated to the Mn^1 and $Mn^{1'}$ centers in μ^2:η^2 fashion, whereas it is located much closer to $Mn^{1'}$ than Mn^1. As seen in Table 1, an electron transfer from the O^1 and $O^{1'}$ oxo ligands to the "distal" Mn^2 and $Mn^{2'}$ centers, started in **TS1**, is completed in the product **II**: all four of its Mn centers are now in oxidation state 3+, each bearing about four unpaired electrons. The spins of these Mn centers are ferromagnetically coupled. The resulting O_2^{2-} ($O^1-O^{1'}$) unit bears just 0.15e of β-spin density, and O^2 and $O^{2'}$ centers bear together 0.15e of β-spin density as well. The antiferromagnetic coupled ^9A state of the II lies only 1.3 (0.4) kcal/mol higher in energy (see Table 1).

In summary, during the **I** → **TS1** → **II** process, four Mn−O bonds (specifically the Mn^1-O^1, $Mn^1-O^{1'}$, Mn^2-O^1, and $Mn^2-O^{1'}$) are weakened/broken, the O−O (specifically $O^1-O^{1'}$)

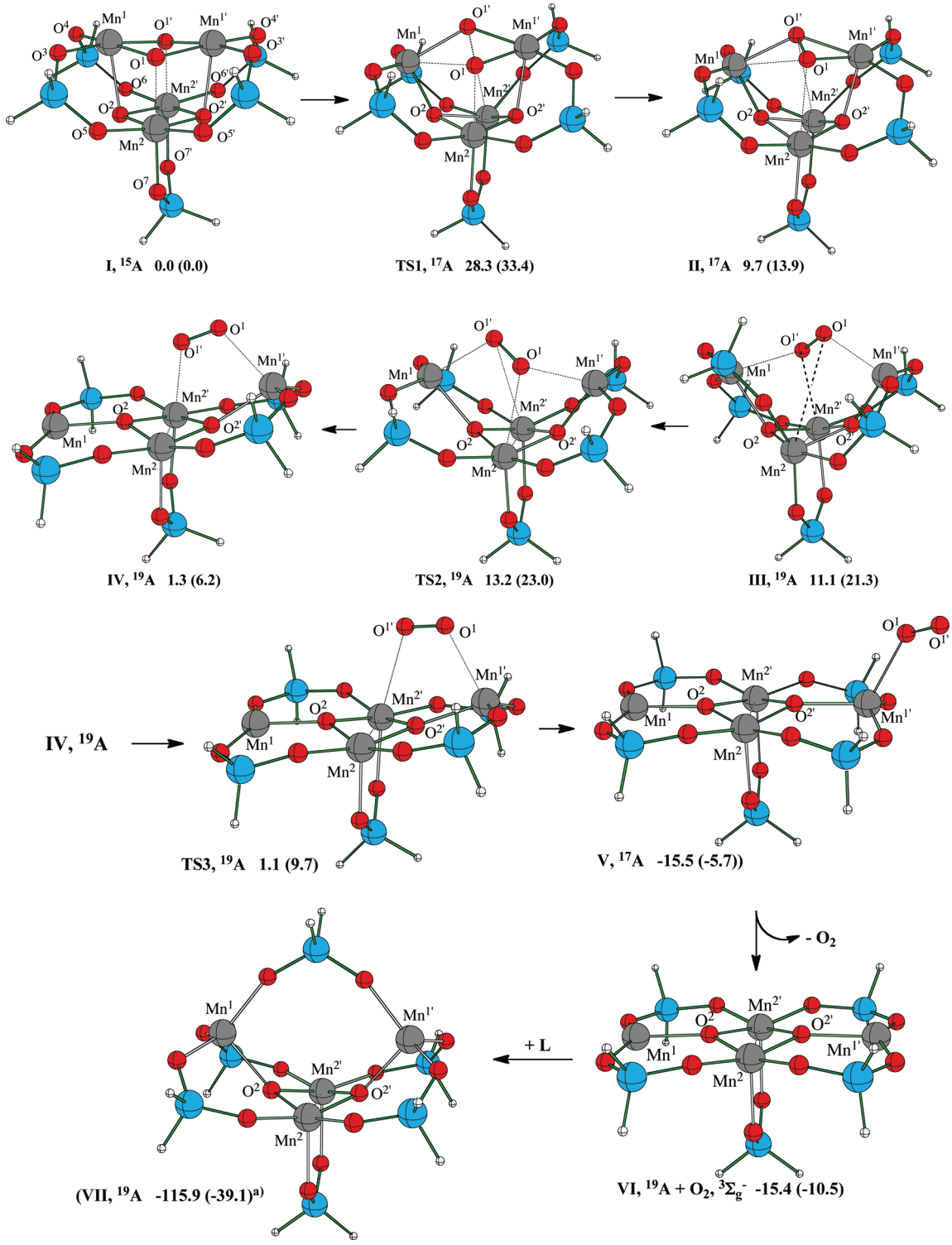

Figure 2. Optimized structures of the reactants, transition states, intermediates, and products for O_2 formation and release from the cationic $Mn_4O_4L_5^+$ species, **I**. Table 2 includes the calculated important geometry parameters for these species. Their relative energies (relative to structure **I**) are given in kcal/mol. (a) This is an energy (in kcal/mol) of the reaction **VI** + L → **VII**.

bond is formed, and the resulting O_2^{2-}-unit is strongly coordinated to the $Mn^{1'}$-center in η^2-fashion. One should also emphasize that during this process, the ground electronic states of the calculated structures change from ^{15}A (reactant **I**) to ^{17}A (product **II**). In this first step of the reaction the Mn^2 and $Mn^{2'}$ centers of **I** are reduced by one electron each (namely, the oxidation states of Mn^2 and $Mn^{2'}$ change from 4+ to 3+), and the required electrons are provided by the two oxo centers, O^1 and $O^{1'}$. In other words, the electrons from the O^1 and $O^{1'}$ centers, located in the top half of the Mn_4O_4-core, transfer to the Mn centers (henceforth "distal"), located at the bottom half of the Mn_4O_4-core, that result in formation of the $O^1-O^{1'}$ bond.

C. Elimination of the Resulting O_2 Molecule and Formation of the Reduced $Mn_4O_2L_5^+$ Species. As mentioned above, in intermediate **II** the resulting O_2 unit has only 0.15 e β-spin and all Mn-centers are in the 3+ oxidation state (with ca. four unpaired α-spins at each) and are ferromagnetically coupled leading to the ^{17}A ground electronic state. From this intermediate

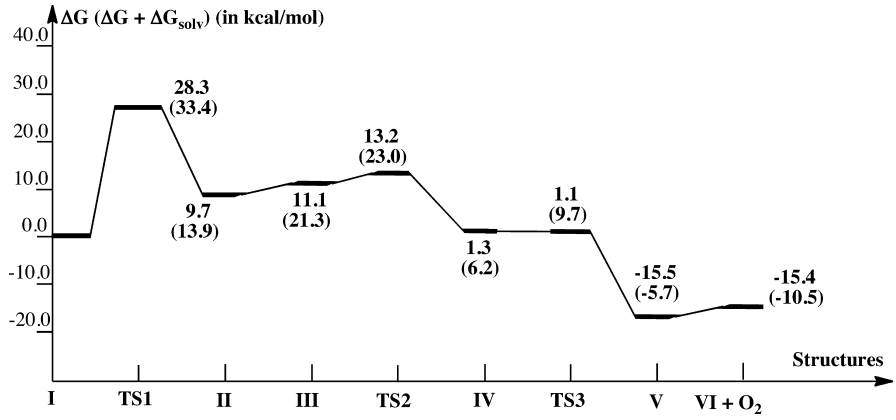

Figure 3. Schematic presentation of the potential energy surface for O_2 formation and release from $Mn_4O_4L_5^+$, **I**.

the reaction (see Scheme 1) proceeds via the O_2 molecule elimination, which involves multiple intermediates and transition states. Initially, the $Mn^1-O_2^{2-}$ and $Mn^{1'}-O_2^{2-}$ bonds are weakened to form complex **III.** The ground electronic state of **III** is found to be ^{19}A. As seen in Table 1, during this process the Mn^1 center is reduced. The required electron is provided by the O_2^{2-} ($O^1O^{1'}$) unit. Indeed, now, in the ^{19}A ground state of the complex **III**, the $O^1O^{1'}$ unit bears 1.13e of α-spin, the Mn^1 center is in the 2+ oxidation state and bears 4.77e of α-spin, and other three Mn centers keep their initial (from complex **II**) 3+ oxidation states and bear about 4 electrons of α-spin each. On the basis of the geometry (the $O^1-O^{1'}$ bond distance reduced from 1.50 to 1.38 Å) and electronic structure criteria, the $O^1O^{1'}$ moiety in **III** can be consider to be a superoxide (O_2^-) ligand Thus, during the **II** → **III** transformation, one-electron reduction of the Mn_4-core (specifically $Mn^{1'}$) occurs by the previously formed O_2^{2-} ($O^1-O^{1'}$) fragment, which becomes O_2^- in the product, **III**.

Since the reactant **II** and product **III** of this step have different ground electronic states, ^{17}A and ^{19}A, respectively, the **II** → **III** transformation is expected to proceed via a spin-crossing pathway. Unfortunately, all our attempts to localize a transition state separating these two complexes failed. However, our extensive search for this transition state indicated a small energy barrier separating the two complexes. The **II** → **III** transformation is found to be endothermic by 1.4 kcal/mol in the gas phase. However, its endothermicity increases to (7.4) kcal/mol in aqueous solution.

As seen in Figure 2 and Table 2, the $O^1O^{1'}$ in **III** unit is weakly coordinated to the Mn^1 and $Mn^{1'}$ centers in an μ^2:η^2 fashion: the calculated $Mn^1-O^{1'}$ and $Mn^{1'}-O^1$ bond distances are long, 2.27 and 2.20 Å, respectively. Complex **III** further transforms to the "open-butterfly" structure **IV**, another weakly coordinated O_2^- complex (with the O_2^- fragment now located between the $Mn^{2'}$ and $Mn^{1'}$ centers), via the transition state **TS2**, which is confirmed to be a real transition state with one imaginary frequency of 212 cm^{-1}. The calculated barrier height at **TS2** is very small, 2.1 (1.7) kcal/mol. The geometry of **TS2** looks very similar to that of the structure **III**: the major difference is the rotation of $O^1O^{1'}$ unit around the axis directed along the $Mn^1-Mn^{1'}$ distance. As a result, the Mn^2-O^1 distance shortens by 1.07 Å, and the $Mn^{2'}-O^{1'}$ distance elongates by 0.99 Å. The Mulliken analysis shows that the $O^1O^{1'}$ unit in **TS2** bears a smaller amount of unpaired electron density than in **III** (by 0.21e), the Mn^1 center still bears about five unpaired electrons, the $Mn^{2/2'}$ centers have about four unpaired electrons each, but the $Mn^{1'}$ center has 0.47e of α-spin density more than that in the species **III**, and the O^2 and $O^{2'}$ centers acquire 0.15e and 0.20e of β-spin density, respectively (Table 1). Thus, in **TS2**, the $Mn^{2/2'}$ centers are still in oxidation state 3+, Mn^1 center has oxidation state 2+, and $Mn^{1'}$ center should be considered as having an intermediate oxidation state 3+/2+. The $O^1O^{1'}$ unit is still considered to be a O_2^- moiety. Thus, in **TS2** another 1-electron reduction/oxidation of Mn/O starts: the electron is transferred from the O_2^- fragment to $Mn^{1'}$ center.

Passing over **TS2** completes the fourth (in total) electron transfer process and leads to formation of the "open-butterfly" flattened structure **IV**, in which the $O^1O^{1'}$ unit is coordinated to the $Mn^{2'}$ and $Mn^{1'}$ centers with relatively long $Mn^{2'}-O^{1'}$ and $Mn^{1'}-O^1$ bond distances, 2.17 and 2.31 Å, respectively. It should be noted that the calculations show the existence of another isomer of **IV**, one in which the $O^1O^{1'}$ unit is coordinated to the Mn^2 and $Mn^{1'}$ centers. Apparently, there is a small energy barrier that interconverts these isomers of **IV**. In **IV**, the $O^1-O^{1'}$ bond distance is shortened by 0.06 Å compared to **III** and becomes closer to the calculated value of 1.27 Å for the free O_2 molecule.

The Mulliken analysis shows that in **IV** the $O^1O^{1'}$ unit bears 0.56e (α-spin), which is significantly smaller than 1.13e in intermediate **III** or 0.92e in transition state **TS2**. The Mn^1 and $Mn^{1'}$ centers bear about five unpaired electrons each (α-spin), thus having oxidation state 2+; the Mn^2 center bears about four unpaired electrons (oxidation state 3+); and, interestingly, $Mn^{2'}$ bears about 3.5e compared to 3.87e in intermediate **III** (Table 1), thus having an intermediate oxidation state 3+/4+. Thus, the overall **II** → **III** → **TS2** → **IV** process is another two-electron oxidation/reduction process, during which the O_2^{2-} dianion converts to the neutral O_2 molecule, and two more Mn centers (namely, Mn^1 and $Mn^{1'}$) are reduced from oxidation state 3+ to 2+. This process is calculated to be exothermic by 8.4 (7.7) kcal/mol, and occurs with an insignificant energy barrier, i.e. this process is expected to be quite facile process. One should note that with formation of complex **IV**, the required 4-electron oxidation/reduction of Mn_4O_4-core is completed.

The process starting from the resulting complex **IV** is a simple O_2 elimination and does not involve any electron transfer. After **IV** the reaction proceeds via transition state **TS3** to form complex **V** in which the O_2 moiety is coordinated in η^1-fashion by its O^1 atom to the $Mn^{1'}$ center of the almost flat $Mn_4O_2L_5^+$ species (Figure 1). The ground electronic state of **TS3**, similar to that of **IV**, is found to be the ^{19}A state. The calculated barrier height at **TS3** is 0.2 (3.5) kcal/mol. This is consistent with a small, 46 cm^{-1}, imaginary frequency corresponding to the reaction coordinate. The $O^1-O^{1'}$ bond distance in **TS3** is 0.02 Å longer than the calculated value for the free O_2 molecule (see Table 2). The $O^1O^{1'}$ unit in **TS3** is weakly coordinated to the Mn_4O_2 core, with $Mn^{1'}-O^1$ and $Mn^{2'}-O^{1'}$ bond distances being

2.70 and 2.39 Å, respectively. The Mulliken spin density analysis shows that the $O^1O^{1'}$ unit in **TS3** bears just 0.18e of α-spin density, whereas $Mn^{1/1'}$ and $Mn^{2/2'}$ centers bear about five and four unpaired electrons, respectively (Table 1).

The resulted intermediate **V** has a ^{17}A ground state, in which the O_2 unit has 1.91e of β-spin density, $Mn^{1/1'}$ centers have almost 5 unpaired α-spins each, and $Mn^{2/2'}$ centers have almost 4 unpaired α-spins each. Thus, the spins of the $O^1O^{1'}$ fragment are antiferromagnetically coupled with the spins of the Mn centers. The reaction **IV** → **TS3** → **V**, during which the oxidation states of the Mn and O centers of the Mn_4O_4-core remain the same, was calculated to be exothermic by 16.8 (11.9) kcal/mol.

Elimination of the triplet O_2 molecule from **V** leads to the flat $Mn_4O_2L_5^+$ species **VI** with a ^{19}A ground state (Figure 2). This step, that is, **V** → **VI** + $\mathbf{O_2}$, was calculated to be slightly, by 0.1 kcal/mol, endothermic in the gas phase, but by (4.8) kcal/mol exothermic in water. The overall reaction **I** → **TS1** → **II** → **III** → **TS2** → **IV** → **TS3** → **V** → **VI** + $\mathbf{O_2}$ was found to be exothermic by 15.4 (10.5) kcal/mol.

Coordination of the $L^- = H_2PO_2^-$ ligand to complex **VI**, which is found to be exothermic by 115.9 (39.1) kcal/mol, leads to formation of the "butterfly" structure **VII**. The **VI** + L → **VII** transformation does not significantly change the spin distribution of **VI**, but it becomes bent (from the flattened structure).

The potential energy surface (PES) for O_2 abstraction from the cationic **I** species is given in Figure 3.

IV. Conclusions

From the discussion above and Figure 3, one can draw the following conclusions:

(1) Dissociation of the $L^- = H_2PO_2^-$ ligand from species **6** (a) makes the Mn_4O_4-core more compact, (b) significantly shortens the $O^1-O^{1'}$ distance and consequently facilitates $O^1-O^{1'}$ bond formation, and (c) does not significantly change spin distribution in the Mn_4O_4-core.

(2) The $O^1-O^{1'}$ single bond formation in reactant **I**, that is, the reaction **I** → **TS1** → **II**, is a two-electron oxidation/reduction process that proceeds with a 28.3 (33.4) kcal/mol energy barrier at **TS1** and is endothermic by 9.7 (13.9) kcal/mol. This is the rate-determining step of entire reaction, during which two oxo ligands (namely, O^1 and $O^{1'}$) located at the top Mn_2O_2 half of the Mn_4O_4 core, reduce the Mn^2 and $Mn^{2'}$ centers of **I** (from 4+ to 3+) that are located in the bottom Mn_2O_2 half of the Mn_4O_4 core.

(3) The next two-electron oxidation (i.e., the $O^1-O^{1'}$ double bond formation) occurs during the **II** → **III** → **TS2** → **IV** transformation, which is calculated to be exothermic by 8.4 (7.7) kcal/mol. This occurs with insignificant energy barriers and involves "dancing" of the O_2^{2-} fragment (i.e., the $O^1O^{1'}$ formed in the previous step of the reaction) between the Mn^1 and Mn^2/$Mn^{2'}$ centers, while maintaining strong coordination to the $Mn^{1'}$-center. Thus, as a result of this overall four-electron oxidation/reduction process, the Mn-centers of the Mn_4-core of **I** have transformed from {Mn^1(III)-$Mn^{1'}$(III)-Mn^2(IV)-$Mn^{2'}$(IV)} to {Mn^1(II)-$Mn^{1'}$(II)-Mn^2(III)-$Mn^{2'}$(III)} in **IV**.

(4) The overall reaction **I** → **TS1** → **II** → **III** → **TS2** → **IV** → **TS3** → **V** → **VI** + $\mathbf{O_2}$ is found to be exothermic by 15.4 (10.5) kcal/mol. Coordination of the $L^- = H_2PO_2^-$ ligand to complex **VI** is a highly exothermic process, 115.9 (39.1) kcal/mol, and leads to formation of the "butterfly" structure **VII**.

Acknowledgment. The present research is supported by grant DE-FG02-03ER15461 of U.S. Department of Energy. The use of computational resources at the Cherry Emerson Center for Scientific Computation is also acknowledged.

Supporting Information Available: Cartesian coordinates of all structures discussed in the paper. This material is available free of charge via the Internet at http://pubs.acs.org.

References and Notes

(1) Lewis, N. S.; Nocera, D. G. *Proc. Natl. Acad. Sci. (USA)* **2006**, *103*, 15729–15735.
(2) Eisenberg, R.; Gray, H. B. *Inorg. Chem.* **2008**, *47*, 1697–1699, and references therein, and the entire issue.
(3) Gersten, S. W.; Samuels, G. J.; Meyer, T. J. *J. Am. Chem. Soc.* **1982**, *104*, 4029–4030.
(4) Gilbert, J. A.; Eggleston, D. S.; Wyatt, R. M., Jr.; Geselowitz, D. A.; Gersten, S. W.; Hodgson, D. J.; Meyer, T. J. *J. Am. Chem. Soc.* **1985**, *107*, 3855–3864.
(5) Comte, P.; Nazeeruddin, M. K.; Rotzinger, F. P.; Frank, A. J.; Grätzel, M. *J. Mol. Catal.* **1989**, *52*, 63–84.
(6) Schoonover, J. R.; Ni, J.; Roecker, L.; White, P. S.; Meyer, T. J. *Inorg. Chem.* **1996**, *35*, 5885–5892.
(7) Wada, T.; Tsuge, K.; Tanaka, K. *Angew. Chem., Int. Ed.* **2000**, *39*, 1479–1482.
(8) Sens, C.; Romero, I.; Rodríguez, M.; Llobet, A.; Parella, T.; Benet-Buchholz, J. *J. Am. Chem. Soc.* **2004**, *126*, 7798–7799.
(9) Hurst, J. K. *Coord. Chem. Rev.* **2005**, *249*, 313–328.
(10) Zong, R.; Thummel, R. *J. Am. Chem. Soc.* **2005**, *127*, 12802–12803.
(11) Liu, F.; Concepcion, J. J.; Jurss, J. W.; Cardolaccia, T.; Templeton, J. L.; Meyer, T. J. *Inorg. Chem.* **2008**, *47*, 1727–1752.
(12) Hurst, J. K.; Cape, Jonathan, L.; Clark, A. E.; Das, S.; Qin, C. *Inorg. Chem.* **2008**, *47*, 1753–1764.
(13) Deng, Z.; Tseng, H.-W.; Zong, R.; Wang, D.; Thummel, R. *Inorg. Chem.* **2008**, *47*, 1835–1848.
(14) Romero, I.; Rodríguez, M.; Sens, C.; Mola, J.; Kollipara, M. R.; Francàs, L.; Mas-Marza, E.; Escriche, L.; Llobet, A. *Inorg. Chem.* **2008**, *47*, 1824–1834.
(15) Concepcion, J. J.; Jurss, J. W.; Templeton, J. L.; Meyer, T. J. *Proc. Nat. Acad. Sci.* **2008**, *105*, 17632–17635.
(16) Concepcion, J. J.; Jurss, J. W.; Templeton, J. L.; Meyer, T. J. *J. Am. Chem. Soc.* **2008**, *130*, 16462–16463.
(17) Sala, X.; Romero, I.; Rodriguez, M.; Escriche, L.; Llobet, A. *Angew. Chem., Int. Ed.* **2009**, *48*, 2842–2852.
(18) Romain, S.; Bozoglian, F.; Sala, X.; Llobet, A. *J. Am. Chem. Soc.* **2009**, *131*, 2768–2769.
(19) Xu, Y.; Åkermark, T.; Gyollai, V.; Zou, D.; Eriksson, L.; Duan, L.; Zhang, R.; Åkermark, B.; Sun, L. *Inorg. Chem.* **2009**, *48*, 2717–2719.
(20) Rotzinger, F. P.; Munavalli, S.; Comte, P.; Hurst, J. K.; Gratzel, M.; Pern, F.-J.; Frank, A. J. *J. Am. Chem. Soc.* **1987**, *109*, 6619–6626.
(21) Rüttinger, W.; Dismukes, G. C. *Chem. Rev.* **1996**, *97*, 1–24.
(22) Limburg, J.; Vrettos, J. S.; Liable-Sands, L. M.; Rheingold, A. L.; Crabtree, R. H.; Brudvig, G. W. *Science* **1999**, *283*, 1524–1527.
(23) Chen, H.; Faller, J. W.; Crabtree, R. H.; Brudvig, G. W. *J. Am. Chem. Soc.* **2004**, *126*, 7345–7349.
(24) Tagore, R.; Chen, H.; Zhang, H.; Crabtree, R. H.; Brudvig; Gary, W. *Inorg. Chim. Acta* **2007**, *360*, 2983–2989.
(25) Tagore, R.; Crabtree, R. H.; Brudvig, G. W. *Inorg. Chem.* **2007**, *46*, 2193–2203.
(26) Tagore, R.; Crabtree, R. H.; Brudvig, G. W. *Inorg. Chem.* **2008**, *47*, 1815–1823.
(27) Maneiro, M.; Ruettinger, W. F.; Bourles, E.; McLendon, G. L.; Dismukes, G. C. *Proc. Natl. Acad. Sci. U.S.A.* **2003**, *100*, 3707–3712.
(28) Siegbahn, P. E. M. *Inorg. Chem.* **2008**, *47*, 1779–1786.
(29) Yagi, M.; Kaneko, M. *Chem. Rev.* **2001**, *101*, 21–35.
(30) Brimblecombe, R.; Kolling, D. R. J.; Bond, A. M.; Dismukes, G. C.; Swiegers, G. F.; Spiccia, L. *Inorg. Chem.* **2009**, *48*, 7269–7279.
(31) Brimblecombe, R.; Swiegers, G. F.; Dismukes, G. C.; Spiccia, L. *Angew. Chem., Int. Ed.* **2008**, *47*, 7335–7338.
(32) (a) Wu, J.-Z.; De Angelis, F.; Carrell, T. G.; Yap, G. P. A.; Sheats, J.; Car, R.; Dismukes, G. C. *Inorg. Chem.* **2006**, *45*, 189–195. (b) Wu, J.-Z.; Sellitto, E.; Yap, G. P. A.; Sheats, J.; Dismukes, G. C. *Inorg. Chem.* **2004**, *43*, 5795–5797. (c) Carrell, T. G.; Bourles, E.; Lin, M.; Dismukes, G. C. *Inorg. Chem.* **2003**, *42*, 2849–2858.
(33) Yagi, M.; Wolf, K. V.; Baesjou, P. J.; Bernasek, S. L.; Dismukes, G. C. *Angew. Chem., Int. Ed.* **2001**, *40*, 2925–2928.
(34) Carrell, T. G.; Cohen, S.; Dismukes, G. C. *J. Mol. Cat. A* **2002**, *187*, 3–15.
(35) Brimblecombe, R.; Koo, A.; Dismukes, G. C.; Swiegers, G. F.; Spiccia, L. *J. Am. Chem. Soc.* **2010**, *132*, 2892–2894.
(36) (a) Dismukes, G. C.; Brimblecombe, R.; Felton, G. A. N.; Pryadin, R. S.; Sheats, J. E.; Spiccia, L.; Swiegers, G. F. *Acc. Chem. Res.* **2009**, *42*, 1935–1943. (b) Swiegers, G. F.; Huang, J.; Brimblecombe, R.; Chen, J.;

Dismukes, G. C.; Mueller-Westerhoff, U. T.; Spiccia, L.; Wallace, G. G. *Chem.—Eur. J.* **2009**, *15*, 4746–4759.
(37) McDaniel, N. D.; Coughlin, F. J.; Tinker, L. L.; Bernhard, S. *J. Am. Chem. Soc.* **2008**, *130*, 210–217.
(38) Hull, J. F.; Balcells, D.; Blakemore, J. D.; Incarvito, C. D.; Eisenstein, O.; Brudvig, G. W.; Crabtree, R. H. *J. Am. Chem. Soc.* **2009**, *131*, 8730–8731.
(39) Kunkely, H.; Vogler, A. *Angew. Chem., Int. Ed.* **2009**, *48*, 1685–1687.
(40) Kanan, M. W.; Nocera, D. G. *Science* **2008**, *321*, 1072–1075.
(41) Kanan, M. W.; Surendranath, Y.; Nocera, D. G. *Chem. Soc. Rev.* **2009**, *38*, 109–114.
(42) Lutterman, D. A.; Surendranath, Y.; Nocera, D. G. *J. Am. Chem. Soc.* **2009**, *131*, 3838–3839.
(43) Hoertz, P. G.; Kim, Y.-I.; Youngblood, W. J.; Mallouk, T. E. *J. Phys. Chem. B* **2007**, *111*, 6845–6856.
(44) Ghosh, P. K.; Brunschwig, B. S.; Chou, M.; Creutz, C.; Sutin, N. *J. Am. Chem. Soc.* **1984**, *106*, 4772–4783.
(45) Hammarström, L.; Sun, L.; Åkermark, B.; Styring, S. *Catal. Today* **2000**, *58*, 57–69.
(46) Youngblood, W. J.; Lee, S.-H. A.; Kobayashi, Y.; Hernandez-Pagan, E. A.; Hoertz, P. G.; Moore, T. A.; Moore, A. L.; Gust, D.; Mallouk, T. E. *J. Am. Chem. Soc.* **2009**, *131*, 926–927.
(47) Lehn, J. M.; Sauvage, J. P.; Ziesel, R. *Nouv. J. Chim.* **1979**, *3*, 423–427.
(48) Schoenfeldt, N. J.; Korinda, A. W.; Notestein, J. M. *Chem. Comm* **2010**, *46*, 1640–1642.
(49) Geletii, Y. V.; Botar, B.; Kögerler, P.; Hillesheim, D. A.; Musaev, D. G.; Hill, C. L. *Angew. Chem., Int. Ed.* **2008**, *47*, 3896–3899.
(50) Geletii, Y. V.; Besson, C.; Hou, Y.; Yin, Q.; Musaev, D. G.; Quinonero, D.; Cao, R.; Hardcastle, K. I.; Proust, A.; Kogerler, P.; Hill, C. L. *J. Am. Chem. Soc.* **2009**, *131*, 17360–17370.
(51) Geletii, Y. V.; Huang, Z.; Hou, Y.; Musaev, D. G.; Lian, T.; Hill, C. L. *J. Am. Chem. Soc.* **2009**, *131*, 7522–7523.
(52) Sartorel, A.; Carraro, M.; Scorrano, G.; Zorzi, R. D.; Geremia, S.; McDaniel, N. D.; Bernhard, S.; Bonchio, M. *J. Am. Chem. Soc.* **2008**, *130*, 5006–5007.
(53) Sartorel, A.; Mir, P.; Salvadori, E.; Romain, S.; Carraro, M.; Scorrano, G.; Di Valentin, M.; Llobet, A.; Bo, C.; Bonchio, M. *J. Am. Chem. Soc.* **2009**, *131*, 16051–16053.
(54) Besson, C.; Huang, Z.; Geletii, Y. V.; Lense, S.; Hardcastle, K. I.; Musaev, D. G.; Lian, T.; Proust, A.; Hill, C. L. *Chem. Commun.* **2010**, *46*, 2784–2786.
(55) Yin, Q.; Miles, M. T.; Besson, C.; Geletii, Y. V.; Musaev, D. G.; Kuznetsov, A. E.; Luo, Z.; Hardcastle, K. I.; Hill, C. L. *Science* **2010**, *328*, 342–345.
(56) Cao, R.; Ma, H.; Geletii, Y. V.; Hardcastle, K. I.; Hill, C. L. *Inorg. Chem.* **2009**, *48*, 5596–5598.
(57) Fang, X.; Speldrich, M.; Schilder, H.; Cao, R.; O'Halloran, K. P.; Hill, C. L.; Kogerler, P. *Chem Comm.* **2010**, *46*, 2760–2762.
(58) Chronister, C. W.; Binstead, R. A.; Ni, J.; Meyer, T. J. *Inorg. Chem.* **1997**, *36*, 3814–3815.
(59) Binstead, R. A.; Chronister, C. W.; Ni, J.; Hartshorn, C. M.; Meyer, T. J. *J. Am. Chem. Soc.* **2000**, *122*, 8464–8473.
(60) Yamada, H.; Koike, T.; Hurst, J. K. *J. Am. Chem. Soc.* **2001**, *123*, 12775–12780.
(61) Bartolotti, L. J.; Pedersen, L. G.; Meyer, T. J. *Int. J. Quantum Chem.* **2001**, *83*, 143–149.
(62) Yamada, H.; Siems, W. F.; Koike, T.; Hurst, J. K. *J. Am. Chem. Soc.* **2004**, *126*, 9786–9795.
(63) Hurst, J. K. *Coord. Chem. Rev.* **2005**, *249*, 313–328.
(64) Yang, X.; Baik, M.-H. *J. Am. Chem. Soc.* **2006**, *128*, 7476–7485.
(65) Yang, X.; Baik, M.-H. *J. Am. Chem. Soc.* **2004**, *126*, 13222–13223.
(66) Batista, E. R.; Martin, R. L. *J. Am. Chem. Soc.* **2007**, *129*, 7224–7225.
(67) Muckerman, J. T.; Polyansky, D. E.; Wada, T.; Tanaka, K.; Fujita, E. *Inorg. Chem.* **2008**, *47*, 1787–1802.
(68) Siegbahn, P. E. M. *Inorg. Chem.* **2000**, *39*, 2923–2935.
(69) Siegbahn, P. E. M.; Crabtree, R. H. *J. Am. Chem. Soc.* **1999**, *121*, 117–127.
(70) Siegbahn, P. E. M. *Acc. Chem. Res.* **2009**, *42*, 1871–1880.
(71) Petrie, S.; Stranger, R. *Inorg. Chem.* **2004**, *43*, 5237–5244.
(72) Petrie, S.; Mukhopadhyay, S.; Armstrong, W. H.; Stranger, R. *Phys. Chem. Chem. Phys.* **2004**, *6*, 4871–4877.
(73) Aullon, G.; Ruiz, E.; Alvarez, S. *Chem.—Eur. J.* **2002**, *8*, 2508–2515.
(74) Mitani, M.; Wakamatsu, Y.; Katsurada, T.; Yoshioka, Y. *J. Phys. Chem. A* **2006**, *110*, 13895–13914.
(75) Sproviero, E. M.; Gacson, J. A.; McEvoy, J. P.; Brudvig, G. W.; Batista, V. S. *J. Inorg. Biochem.* **2006**, *100*, 786–800.
(76) Quinonero, D.; Kaledin, A. L.; Kuznetsov, A. E.; Geletii, Y. V.; Besson, C.; Hill, C. L.; Musaev, D. G. *J. Phys. Chem. A* **2010**, *114*, 535–542.
(77) Kuznetsov, A. E.; Geletii, Y. V.; Hill, C. L.; Morokuma, K.; Musaev, D. G. *J. Am. Chem. Soc.* **2009**, *131*, 6844–6854.
(78) Bozoglian, F.; Romain, S.; Ertem, M. Z.; Todorova, T. K.; Sens, C.; Mola, J.; Rodriguez, M.; Romero, I.; Benet-Buchholz, J.; Fontrodona, X.; Cramer, C. J.; Gagliardi, L.; Llobet, A. *Am. Chem. Soc.* **2009**, *131*, 15176–15187.
(79) Jaque, P.; Marenich, A. V.; Cramer, C. J.; Truhlar, D. G. *J. Phys. Chem. C* **2007**, *111*, 5783–5799.
(80) Yang, X.; Hall, M. B. *J. Am. Chem. Soc.* **2010**, *132*, 120–130.
(81) Wang, L.-P.; Wu, Q.; Van Voorhis, T. *Inorg. Chem.* **2010**, *49*, 4543–4553.
(82) Liu, F.; Concepcion, J. J.; Jurss, J. W.; Cardolaccia, T.; Templeton, J. L.; Meyer, T. J. *Inorg. Chem.* **2008**, *47*, 1727–1752.
(83) Tseng, H.-W.; Zong, R.; Muckerman, J. T.; Thummel, R. *Inorg. Chem.* **2008**, *47*, 11763–11773.
(84) Yang, X.; Baik, M.-H. *J. Am. Chem. Soc.* **2008**, *130*, 16231–16240.
(85) Wang, T.; Brudvig, G.; Batista, V. S. *J. Chem. Theory Comput.* **2010**, *6*, 755–760.
(86) Frisch, M. J.; Trucks, G. W.; Schlegel, H. B.; Scuseria, G. E.; Robb, M. A.; Cheeseman, J. R.; Montgomery, J. A., Jr.; Vreven, T.; Kudin, K. N.; Burant, J. C.; Millam, J. M.; Iyengar, S. S.; Tomasi, J.; Barone, V.; Mennucci, B.; Cossi, M.; Scalmani, G.; Rega, N.; Petersson, G. A.; Nakatsuji, H.; Hada, M.; Ehara, M.; Toyota, K.; Fukuda, R.; Hasegawa, J.; Ishida, M.; Nakajima, T.; Honda, Y.; Kitao, O.; Nakai, H.; Klene, M.; Li, X.; Knox, J. E.; Hratchian, H. P.; Cross, J. B.; Bakken, V.; Adamo, C.; Jaramillo, J.; Gomperts, R.; Stratmann, R. E.; Yazyev, O.; Austin, A. J.; Cammi, R.; Pomelli, C.; Ochterski, J. W.; Ayala, P. Y.; Morokuma, K.; Voth, G. A.; Salvador, P.; Dannenberg, J. J.; Zakrzewski, V. G.; Dapprich, S.; Daniels, A. D.; Strain, M. C.; Farkas, O.; Malick, D. K.; Rabuck, A. D.; Raghavachari, K.; Foresman, J. B.; Ortiz, J. V.; Cui, Q.; Baboul, A. G.; Clifford, S.; Cioslowski, J.; Stefanov, B. B.; Liu, G.; Liashenko, A.; Piskorz, P.; Komaromi, I.; Martin, R. L.; Fox, D. J.; Keith, T.; Al-Laham, M. A.; Peng, C. Y.; Nanayakkara, A.; Challacombe, M.; Gill, P. M. W.; Johnson, B.; Chen, W.; Wong, M. W.; Gonzalez, C.; Pople, J. A. *Gaussian 03*, revision C1; Gaussian, Inc.: Wallingford, CT, 2003.
(87) (a) Becke, A. D. *Phys. Rev. A* **1988**, *38*, 3098–3107. (b) Lee, C.; Yang, W.; Parr, R. G. *Phys. Rev. B* **1988**, *37*, 785–789. (c) Becke, A. D. *J. Chem. Phys.* **1993**, *98*, 1372–1380.
(88) (a) Hay, P. J.; Wadt, W. R. *J. Chem. Phys.* **1985**, *82*, 270–283. (b) Hay, P. J.; Wadt, W. R. *J. Chem. Phys.* **1985**, *82*, 299–310. (c) Wadt, W. R.; Hay, P. J. *J. Chem. Phys.* **1985**, *82*, 284–298.
(89) Cances, E.; Mennucci, B.; Tomasi, J. *J. Chem. Phys.* **1997**, *107*, 3032–3041.
(90) *CRC Handbook of Chemistry and Physics*, 86th ed.; Lide, D. R., Ed.; CRC Press: Boca Raton, FL, 2005.
(91) Linstrom, P. J.; Mallard, W. G. *NIST Chemistry WebBook*, NIST Standard Reference Database Number 69, March 2003; National Institute of Standards and Technology: Gaithersburg MD, 20899. Available from: http://webbook.nist.gov.
(92) Nakatsuji, H.; Nakai, H. *Chem. Phys. Lett.* **1992**, *197*, 339–345.

JP105422A